APPLIED MICROBIAL AND CELL PHYSIOLOGY

Metal(loid) oxide (Al₂O₃, Mn₃O₄, SiO₂ and SnO₂) nanoparticles cause cytotoxicity in yeast via intracellular generation of reactive oxygen species

Cátia A. Sousa[1,2,3] · Helena M. V. M. Soares[3] · Eduardo V. Soares[1,2]

Abstract

In this work, the physicochemical characterization of five (Al₂O₃, In₂O₃, Mn₃O₄, SiO₂ and SnO₂) nanoparticles (NPs) was carried out. In addition, the evaluation of the possible toxic impacts of these NPs and the respective modes of action were performed using the yeast *Saccharomyces cerevisiae*. In general, in aqueous suspension, metal(loid) oxide (MOx) NPs displayed an overall negative charge and agglomerated; these NPs were practically insoluble (dissolution < 8%) and did not generate detectable amounts of reactive oxygen species (ROS) under abiotic conditions. Except In₂O₃ NPs, which did not induce an obvious toxic effect on yeast cells (up to 100 mg/L), the other NPs induced a loss of cell viability in a dose-dependent manner. The comparative analysis of the loss of cell viability induced by the NPs with the ions released by NPs (NPs supernatant) suggested that SiO₂ toxicity was mainly caused by the NPs themselves, Al₂O₃ and SnO₂ toxic effects could be attributed to both the NPs and the respective released ions and Mn₃O₄ harmfulness could be mainly due to the released ions. Al₂O₃, Mn₃O₄, SiO₂ and SnO₂ NPs induced the loss of metabolic activity and the generation of intracellular ROS without permeabilization of plasma membrane. The co-incubation of yeast cells with MOx NPs and a free radical scavenger (ascorbic acid) quenched intracellular ROS and significantly restored cell viability and metabolic activity. These results evidenced that the intracellular generation of ROS constituted the main cause of the cytotoxicity exhibited by yeasts treated with the MOx NPs. This study highlights the importance of a ROS-mediated mechanism in the toxicity induced by MOx NPs.

Keywords Esterase activity · Membrane integrity · Oxidative stress · Physicochemical properties of nanomaterials · Toxicity

✉ Helena M. V. M. Soares
  hsoares@fe.up.pt

✉ Eduardo V. Soares
  evs@isep.ipp.pt

[1] Bioengineering Laboratory-CIETI, ISEP-School of Engineering, Polytechnic Institute of Porto, Rua Dr António Bernardino de Almeida, 431, 4249-015 Porto, Portugal

[2] CEB-Centre of Biological Engineering, University of Minho, Campus de Gualtar, 4710-057 Braga, Portugal

[3] REQUIMTE/LAQV, Departamento de Engenharia Química, Faculdade de Engenharia, Universidade do Porto, rua Dr Roberto Frias, s/n, 4200-465 Porto, Portugal

Introduction

The use of nanomaterials, worldwide, has increased highly in the last decades. Metal(loid) oxide (MOx) nanoparticles (NPs) constitute an important group of nanomaterials (Corr 2012; Klaine et al. 2013). The global market of MOx NPs was estimated to be between 280,000 and 1.3 million tons per year, which is led by Asian-Pacific (~34%), North American (~30%) and European (~30%) market (Nanotech 2015). The analysts forecast that the global MOx NP market is growing at a mean annual rate of 9.5% during the period 2016–2020 (Research 2017).

MOx NPs present a wide range of applications being used in electronic devices, optic lenses, medicine (implants, cancer diagnosis, therapy and bioimaging), personal care products, paints, coatings, water treatment, energy storage and fuel cells (Andreescu et al. 2012; Fei and Li 2010; Laurent et al. 2018; Nanotech 2015). Among the different MOx NPs, Al₂O₃,

In_2O_3, Mn_3O_4, SiO_2 and SnO_2 NPs have been widely used. Al_2O_3 NPs are employed due to their chemical stability, mechanical strength and electrical insulation capacity (Nanotech 2015). In_2O_3 NPs are used in batteries as a substitute of mercury, in ceramics and electronics due to their optical and antistatic properties (AzoNano 2018; Laurent et al. 2018; Research 2018). Mn_3O_4 NPs are employed in capacitors because these nanoparticles present superior electrochemical properties (Tian et al. 2013). SiO_2 NPs present unique properties, such as mechanical, catalytic, magnetic and optical properties, which lead them to be used in paints, plastic, ceramics, batteries and cosmetics (Report 2018). Due to their semiconductor, electronic, optical and catalytic properties, SnO_2 NPs can be used in a variety of applications in the industry, such as solar cells, photo catalysis and sensors (Chavez-Calderon et al. 2016).

The increasing use of MOx NPs leads, inevitably, to an augmented concern related to its possible toxicity. Studies in soils showed that Al_2O_3, SiO_2 and SnO_2 NPs had an impact in bacterial and in fungal community (Chai et al. 2015; Chavez-Calderon et al. 2016; McGee et al. 2017). Other studies showed that Al_2O_3, Mn_3O_4 and SiO_2 NPs caused growth inhibition of bacteria (*Escherichia coli* and *Staphylococcus aureus*), algae *(Pseudokirchneriella subcapitata*) and protozoa (*Tetrahymena thermophila* and *Paramecium multimicronucleatum*) and bioluminescence reduction of the bacterium *Vibrio fischeri* (Aruoja et al. 2015; Li et al. 2012). SnO_2 NPs caused a reduction of cell viability and provoked the damage of cell membrane in the bacteria *E. coli* and *Bacillus subtilis* (Chavez-Calderon et al. 2016).

To better understand the toxic modes of action of the MOx NPs, the use of a cell model is crucial. The yeast *Saccharomyces cerevisiae*, a unicellular eukaryotic model, is very useful in toxicological studies as a first screen tool (dos Santos et al. 2012). It is a nonpathogenic microorganism with a fast growth, has the genome completely sequenced (Goffeau et al. 1996), presents some similarities with human cells (Karathia et al. 2011), its use in toxicity studies does not raise ethical questions and limits the utilization of animals.

Despite the emerging commercial importance of NPs, a very limited information has been published regarding the toxicity of the NPs studied in the present work. As far as we know, the toxicity of these NPs remains poorly investigated and their toxicity mechanisms are not elucidated, as well. Taking into account these facts, the main aim of the present work was to evaluate the toxic effects of five NPs (Al_2O_3, In_2O_3, Mn_3O_4, SiO_2, SnO_2) using the yeast *S. cerevisiae* as a cell model. The impact of NPs was tested up to 100 mg/L as it is the maximum limit of concentration, advised by the Organization for Economic Co-operation and Development (OECD), for testing toxicity (OECD 2011). The NPs toxicity was evaluated under growing conditions on yeast-extract-peptone (YEP) broth (growth inhibition assay) or in a buffer

medium (cell viability assay). In order to obtain a mechanistic approach of the toxic impact of NPs on yeast cells, plasma membrane integrity, metabolic activity and intracellular accumulation of reactive oxygen species (ROS) were assessed. To further evaluate the role of the oxidative stress (OS) on the cytotoxicity induced by MOx NPs, yeast cells were co-exposed to NPs and an antioxidant (ascorbic acid). Then, the cell viability, esterase activity and intracellular ROS accumulation were accessed and compared. Together, the studies here presented allow to characterize the possible hazard of these NPs.

Material and methods

NPs characteristics and stock suspension preparation

The main characteristics of Al_2O_3, In_2O_3, Mn_3O_4, SiO_2 and SnO_2 NPs used in the present work (namely, purity, particle size and surface area) can be found in Supplementary Table S.1. The purity of NPs was determined by their digestion with aqua regia, as previously described (Sousa et al. 2018); metal (Al, In, Mn and Sn) content was determined by atomic absorption spectroscopy with flame atomization (AAS-FA) in an Analytik Jena novAA 350 spectrometer (Analytik Jena; Jena, Germany).

NPs stock suspensions at 0.5 g/L were prepared in deionized water. The suspensions were vigorously shaken, sonicated for 15 min in an ultrasonic bath (80–160 W; Bandelin, Sonorex RK 100; Berlin, Germany) and sterilized by UV light, as previously described (Sousa et al. 2018). NPs stock suspensions were stored in the dark for up to 1 month, at 4 °C. Before use, NPs stock suspensions were shaken and sonicated as described above.

Characterization of NPs suspensions in different media

In the characterization of the MOx NPs, the hydrodynamic size (Z-average diameter) and the zeta potential were measured in deionized water (stock suspensions), YEP broth [5 g/L yeast extract (Difco-BD; Franklin Lakes, NJ, USA), 5 g/L peptone (Difco-BD) and 10 g/L glucose (Merck; Darmstadt, Germany)] or in 10 mmol/L 2-(N-morpholino) ethanesulfonic acid buffer (MES, Sigma-Aldrich; St. Louis, MO, USA) with 20 g/L glucose (Merck), pH 6.0. MOx NPs were suspended at a final concentration of 100 mg/L and incubated in the same conditions of the assays with yeast cells, as described below. The Z-average diameter and the zeta potential were measured using a Zetasizer Nano ZS (Malvern Instruments; Malvern, UK), coupled with Zetasizer Software version 7.11, as previously described (Sousa et al. 2018).

MOx NPs agglomeration was also characterized by a sedimentation assay (Aruoja et al. 2015; Hartmann et al. 2013;

OECD [2017]). For this purpose, NPs were suspended in YEP or MES buffer, at a final concentration of 100 mg/L, and agitated at 150 rpm for 24 h, at 30 °C, in the absence of yeast cells. For a given incubation time, the turbidity of the samples was monitored by spectrophotometric measurement of the absorbance at 600 nm, for 60 min.

Dissolution of NPs in different media

The stability of NPs was evaluated by quantifying the metal(-loid)s dissolved in YEP or MES buffer. As control, the metal(loid)s dissolved in deionized water (pH 6.0) were also quantified. NPs were suspended in the different media, at 100 mg/L, and incubated in the conditions described below (yeast exposure conditions). After 24 h, samples were taken and centrifuged at $20,000 \times g$, for 30 min, at 25 °C. Then, Al, In, Mn and Sn ions were determined in the supernatants by AAS-FA. Si was determined by inductively coupled plasma optical emission spectrometry (ICP-OES) in an iCAP 7000 Series Spectrometer (Thermo Fisher Scientific, Cambridge, UK); Si standard stock solution of 1000 mg/L Si was obtained from Sigma-Aldrich.

Strain, medium and growth conditions

The yeast *S. cerevisiae* BY4741 was used in this work. The strain was obtained from EUROSCARF collection (Frankfurt, Germany) and maintained at 4 °C on YEP agar [YEP broth with 20 g/L agar (Merck)].

The pre-cultures were obtained in YEP broth, adjusted to pH 6.0, and incubated at 30 °C, at 150 rpm, for 8 h. The cultures were obtained by inoculating YEP broth with a suitable volume of the pre-culture; then, cells were incubated overnight to an OD_{600} of ∼ 1.0 under the same conditions described above. Yeast cells, in exponential phase of growth, were centrifuged ($2500 \times g$, 5 min), washed twice, resuspended in deionized water, and used in the assays described below.

Yeast exposure conditions

The toxic effects induced by Al_2O_3, In_2O_3, Mn_3O_4, SiO_2 or SnO_2 NPs on yeast cells were evaluated. In addition, the toxic impact caused by the respective metal ions (in the case of Al_2O_3, In_2O_3, Mn_3O_4 and SnO_2 NPs) was compared. The stock solutions of the metals used were $Al(NO_3)_3$ (1000 mg/L, Merck), $In(NO_3)_3$ (1000 mg/L, Sigma-Aldrich), $MnCl_2$ (2000 mg/L, Merck) and $SnCl_4$ (1000 mg/L, Merck). Due to the high affinity of Si to oxygen, the chemical behaviour of Si (a metalloid) is different from the metals (Hirner and Flaßbeck [2005]). Thus, the dissolution of SiO_2, in water, originates the forming of orthosilicic acid, $Si(OH)_4$ (Iler [1978]), which is silicon tetrahedrally co-ordinated to four hydroxyl groups

(Perry et al. [2003]). Therefore, experiences with Si, similar to those performed with metal ions, could not be done.

Yeast cells were exposed to chemicals in YEP broth (yeast growth inhibition assay) or in 10 mmol/L MES buffer, pH 6.0, with 20 g/L glucose (yeast viability assay). In yeast growth inhibition assay, test tubes containing 1.0 mL of double-strength YEP broth was inoculated with yeasts, in exponential phase of growth, at 1×10^6 cells/mL; different concentrations of each NP or the respective metals were also added: 50, 75 and 100 mg/L MOx NPs or 1.25, 3.12, 6.25, 12.5, 25 and 50 mg/L of the respective metals (toxicant final concentrations). The total volume of each assay (2.0 mL) was adjusted with sterile deionized water. Biotic (yeast cells without toxicants) and abiotic controls (NPs suspensions, at the same concentrations used in the biotic assays, in the culture medium, without yeast cells) were also prepared. Cultures and controls were incubated at 30 °C. After 24 h, the optical density at 600 nm was measured and corrected considering the respective abiotic control. The yeast cell response (growth reduction) was evaluated as a function of the concentration of the toxic agent using as comparison the growth of nonexposed cells (biotic control). The test endpoint is the percentage of growth, expressed as cell yield, in a similar way to that proposed by the OECD for the evaluation of the toxicity of chemical substances using algae or cyanobacteria (OECD [2011]); cell yield is defined as the cell concentration at 24 h minus the cell concentration at the start of the assay.

Alternatively (yeast viability assay), cells in exponential phase of growth were suspended (1×10^7 cells/mL) in MES buffer with glucose and incubated without (control) or with the MOx NPs (50, 75 and 100 mg/L) or the respective metals (0.125, 1.25, 3.12, 6.25, 12.5 mg/L), at 30 °C, 150 rpm. The assay was carried out in 100-mL Erlenmeyer flasks with a final volume of 20 mL. After the exposure to toxicants for 24 h, samples were taken (two replicates), serially diluted with sterile deionized water and dispersed over YEP agar surface (from the convenient dilution) in duplicate for each replica. The cultures were incubated for 3–5 days at 30 °C. Colony-forming units (CFUs) per millilitre were determined from the number of colonies formed and the sample dilution. After this period of incubation, no further CFUs appeared. As toxicity end point, the cell viability was determined considering the number of CFU/mL, at zero time, as reference (100%).

The effect concentration (EC) values of the metals in YEP or MES buffer were determined. EC_{10}, EC_{25}, EC_{50}, EC_{75} and EC_{90} values represent the concentration of metal ions that induce the inhibition of 10, 25, 50, 75 or 90%, respectively, of yeast growth in YEP (growth inhibition assay) or the reduction of cell viability in MES buffer (cell viability assay), after 24 h. The EC values were calculated using the linear interpolation method (TOXCALC version 5.0.32, Tidepool Scientific Software; McKinleyville, CA, USA).

The toxic effects of MOx NPs supernatants were also evaluated. For this purpose, yeast cells were exposed to 100 mg/L MOx NPs in MES buffer with glucose, in 100-mL Erlenmeyer flasks. Cell suspensions were agitated at 150 rpm, at 30 °C. After 24 h of incubation, cells were harvested by centrifugation (20,000×g, 30 min, 25 °C) and the clear supernatants carefully collected. Then, yeast cells in exponential phase of growth at 1×10^7 cells/mL were exposed to MOx NPs supernatants, in 100-mL Erlenmeyer flasks. Cell suspensions were incubated at 30 °C, 150 rpm, for 24 h and the viability determined as described above.

The influence of L-ascorbic acid (AA), an antioxidant, on MOx NPs toxicity was evaluated by pre-incubation of yeasts, in exponential phase of growth, at 1×10^7 cells/mL, in MES buffer with glucose and 10 mmol/L AA (Merck) for 30 min before the exposure to MOx NPs. Cell suspensions were incubated in the same conditions described above. After 24 h of incubation, cell viability was evaluated as described above.

Staining procedures

Cell membrane integrity was evaluated using propidium iodide (PI, Sigma-Aldrich). Cells were exposed to 100 mg/L MOx NPs, for 24 h, at 30 °C, as described above. Then, cells (1×10^7/mL) were incubated with 4.5 μmol/L PI, for 10 min at room temperature, in the dark. As positive control (cells with disrupted membrane), yeasts were heated at 65 °C, during 1 h. Cells were analysed, using an epifluorescence microscope (Leica Microsystems; Wetzlar GmbH, Germany) equipped with a HBO 100 mercury lamp and the I3 filter set from Leica. In each condition tested, at least 200 cells were counted, in duplicate (total ≥ 400 cells) in randomly selected microscope fields.

Metabolic activity of yeast cells was assessed using the fluorescent dye fluorescein diacetate (FDA, Sigma-Aldrich) or 2-chloro-4-(2,3-dihydro-3-methyl-(benzo-1,3-thiazol-2-yl)-methylidene)-1-phenylquinolinium iodide (FUN-1, Molecular Probes, Invitrogen; Eugene, OR, USA). After exposure to MOx NPs for 24 h, as described above, yeast cells (1×10^7/mL) were incubated with 10 μmol/L FDA, for 20 min, in 10 mmol/L PBS buffer (pH 7.0) or with 0.2 mmol/L FUN-1 for 30 min, in 10 mmol/L 4-(2-hydroxyethyl)-1-piperazineethanesulfonic acid (HEPES) buffer (Sigma-Aldrich), pH 7.2, with 20 g/L glucose, in the dark, at room temperature. As negative control (cells without metabolic activity), yeasts were heated at 65 °C, during 1 h. Cells were analysed by fluorescence microscopy, as described above, for cell membrane integrity. Hydrolysis of FDA (esterase activity) was also quantified. After exposure to MOx NPs, cells (1×10^7/mL) were mixed with 10 μmol/L FDA, placed in quadruplicate in 96-well flat microplate and incubated for 40 min, at 25 °C, in the dark. Fluorescence (in relative fluorescence units (RFUs)) was quantified in a microplate reader

at fluorescence excitation wavelength of 485/14 nm and an emission of 535/25 nm (PerkinElmer, VICTOR3; Turku, Finland).

Intracellular generation of ROS was monitored incubating the yeasts in MES buffer with glucose, at 1×10^7 cells/mL, with 20 μmol/L 2′,7′-dichlorodihydrofluorescein diacetate (H$_2$DCFDA, Sigma-Aldrich), at 25 °C for 10 min. Then, cells were exposed to 100 mg/L MOx NPs at 25 °C, in the dark. After 24 h, cells were placed in quadruplicate in 96-well flat microplate and the fluorescence was measured as described for esterase activity (hydrolysis of FDA).

For the determination of ROS in abiotic conditions, H$_2$DCFDA was deacetylated to H$_2$DCF as previously described (Aruoja et al. 2015). MOx NPs were incubated in MES buffer with glucose for 24 h, in the same conditions of the biotic assays. Then, samples (100 μL) were mixed with equal volume of 52 μmol/L H$_2$DCF solution, incubated for 45 min in the dark at 25 °C and the fluorescence quantified in a microplate reader as described above. Blank and positive control were prepared by replacing the sample by equal volume of MES or 26 μmol/L H$_2$O$_2$, respectively. Abiotic ROS was expressed as the ratio of fluorescence of the samples/fluorescence of the blank.

Microscopy

Samples were observed under an epifluorescence microscope equipped with a HBO 100 mercury lamp and the I3 filter set from Leica. Images were captured by Leica DC 300F camera (Leica Microsystems, Heerbrugg, Switzerland) and processed using Leica IM 50-image software.

Reproducibility of the results and statistical analysis

Z-average diameter and zeta potential measurements were determined in duplicate; in each determination, at least ten measurements were performed. All others studies were repeated at least three times, in duplicate ($n \geq 6$). The data reported are mean values ± standard deviation (SD). The mean values were subjected to unpaired t test or one-way ANOVA followed by Tukey-Kramer multiple comparison method; P values < 0.05 were considered statistically significant.

Results

Characterization of NPs suspended in different media

The characteristics of the MOx NPs studied, namely purity, particle size (in powder) and surface area, are presented in the Supplementary Table S1. To further characterize the main physicochemical properties of the NPs suspended in different media (MES buffer with glucose or YEP broth), the following

properties were evaluated: agglomeration (Z-average diameter), surface charge (zeta potential) and solubility (quantification of the metal(loid) dissolved from the NPs). The assays were performed in the absence of yeast cells but in the same conditions of the biotic assays (with yeast cells). For comparative purposes, NPs were suspended in deionized water and the same properties were evaluated.

At zero time (immediately after the suspension in a given medium), the NPs studied, except SnO_2, presented a hydrodynamic size (Z-average diameter), in aqueous media tested, between 600 and 1400 nm (Fig. 1a). Since the NPs tested, when in powder, presented a size < 100 nm, according to the manufacturers (Supplementary Table S1), these results suggest an immediate agglomeration of the NPs, when suspended in aqueous media. The Z-average diameter of In_2O_3, Mn_3O_4 and SiO_2 NPs was similar, in all media tested. The Z-average

diameter of Al_2O_3, in MES buffer, and SnO_2 in both media (YEP or MES buffer) was higher than in deionized water (Fig. 1a). The agglomeration of the NPs increased through the 24 h of incubation period, in both media, being particularly notorious in MES buffer (Fig. 1a). After 24 h, the agglomerates of Al_2O_3, In_2O_3, Mn_3O_4 and SnO_2 NPs could be seen with the naked eye in MES buffer (Supplementary Fig. S1). These observations were further confirmed through the measurement of NPs sedimentation profiles (Supplementary Fig. S2). In YEP, MOx NPs were more stable, which was translated by a lower sedimentation capacity over time (Supplementary Fig. S2); in this medium, the NPs agglomeration was not evident and the formation of agglomerates could not be seen with the naked eye.

All NPs studied presented a negative zeta potential (between − 9 and − 26 mV), except Al_2O_3 in water and in MES

Fig. 1 Nanoparticle properties in aqueous suspension. NPs were suspended at 100 mg/L in water, YEP or 10 mmol/L MES buffer, in the absence of yeast cells, and were incubated at 150 rpm for 24 h. **a** Z-average diameter. **b** Zeta potential. **c** Dissolved metal(loid) from the NPs after 24 h of incubation. The data represent the mean values of at least three independent experiments, performed in duplicate ($n \geq 6$); standard deviations are presented (vertical error bars)
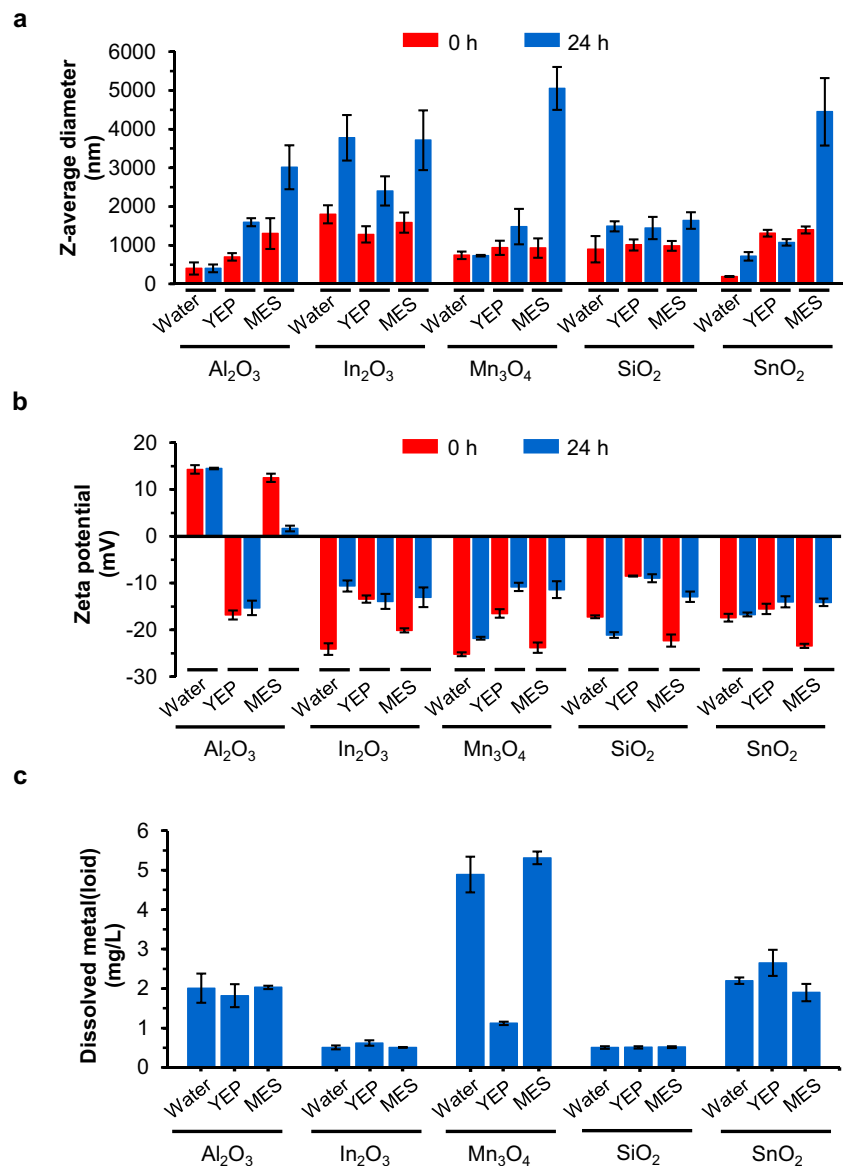
buffer (~ 14 mV) (Fig. 1b). For all NPs, the zeta potential values remained similar or become less negative after 24 h of incubation (-9 to -22 mV), except Al_2O_3 in MES buffer which become less positive (~ 2 mV) and SiO_2 in water which become more negative (-21 mV). These results indicate that NPs formed relatively instable suspensions, which is compatible with the observed agglomeration.

The amount of metal(loid) released from the NPs, in the absence of yeast cells, in the different media, was low (< 6 mg/L) (Fig. 1c). Similar results were observed, in YEP broth or MES buffer, in the presence of yeasts (Supplementary Fig. S3), which suggests that the presence of cells did not interfere with NPs dissolution. These results indicated that the NPs were poorly soluble ($< 8\%$) in MES buffer or YEP broth (Supplementary Table S2).

Impact of the NPs and respective ions on the growth and cell viability

As a first approach, the toxic effect of the NPs over the yeast *S. cerevisiae* was assessed through a 24-h growth inhibition assay, in rich medium (YEP). The presence of the NPs did not affect, significantly, the yeast growth (Fig. 2a). As reported above (Fig. 1c), Al_2O_3, In_2O_3, Mn_3O_4 and SnO_2 NPs release metal ions (NPs dissolution). Thus, for comparative purposes, the effect of the respective metal ions on yeast growth was also

evaluated. Aluminium, indium and tin presented similar growth inhibition profiles (Fig. 2b), which was translated by similar 24-h EC_{50} values (10–13 mg/L) (Supplementary Table S3). Manganese was the less toxic (Fig. 2b), with a 24-h EC_{50} value of 21 mg/L (Supplementary Table S3).

Another strategy to evaluate the NPs toxicity consisted in the incubation of yeast cells with the chemicals, in a buffer (10 mmol/L MES buffer, at pH 6.0, containing 20 g/L glucose). NPs toxicity was evaluated through a clonogenic assay: determination of the ability of the NP-exposed yeasts to form colonies on YEP agar, without toxicant. Except In_2O_3, the other MOx NPs induced a significant loss of cell viability, in a dose-dependent manner (Fig. 2c). The exposure of yeast cells to 100 mg/L of Al_2O_3, Mn_3O_4, SiO_2 and SnO_2 NPs, for 24 h, reduced the cell viability to 50–70% (Fig. 2c). The metal ions correspondent to the NPs (Al, In, Mn and Sn) induced the loss of cell viability (Fig. 2d) and displayed 24-h EC_{50} values between 0.8 and 2.7 mg/L (Supplementary Table S3). These values were about ten times lower that those observed in rich medium (YEP) (Supplementary Table S3).

Where does the toxicity of the NPs come from?

To investigate whether the toxicity observed was due to the nanoparticles, to the chemical species released (NPs solubilization) or to the combination of both, the loss of cell viability

Fig. 2 Impact of the nanoparticles and respective metal ions on yeast growth and cell viability. Yeast cells were exposed to the different toxicants in YEP broth (**a**, **b**) or in MES buffer (**c**, **d**), and the growth (growth inhibition assay) or the cell viability (colony forming unit (CFU) counting) was assessed after 24 h. The data are presented as mean values from at least three independent experiments performed in duplicate ($n \geq 6$); standard deviations are presented (vertical error bars). Mean values are significantly different: *$P < 0.05$ in comparison with untreated cells (control); unpaired *t* test
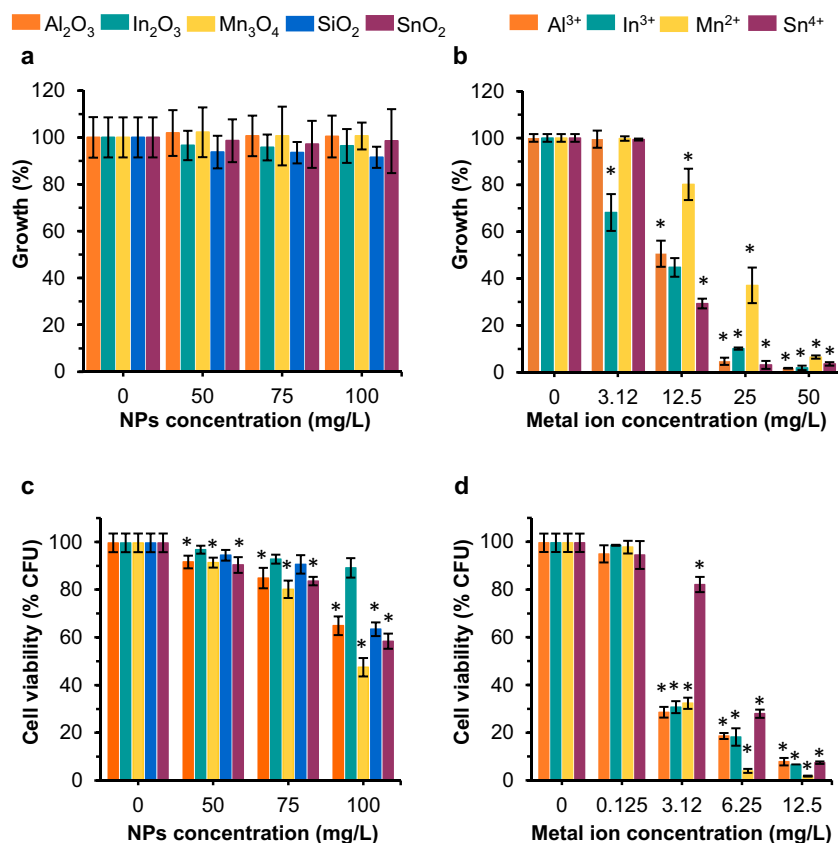
induced by the NPs at 100 mg/L was compared with the toxicity associated to the respective supernatants, which contained the metal(loid)s released by the NPs. The comparative analysis revealed that the toxicity of SiO_2 NPs was mainly caused by the NPs themselves, as the supernatant had no impact on the cell viability (Fig. 3). For both Al_2O_3 and SnO_2 NPs, the toxicity was higher than the corresponding supernatants (Fig. 3), which indicated that the NPs contributed, partially, to the observed toxicity. Thus, for Al_2O_3 and SnO_2 NPs, the loss of yeast cell viability could be attributed to both the NPs and the respective released ions from the NPs. Mn_3O_4 NP supernatant had a higher toxicity effect than the NPs, which suggested that the toxicity of the NPs can be mainly caused by the released Mn ions while the contribution of the Mn_3O_4 NPs to the loss of cell viability could be, practically, neglected (Fig. 3).

The assessment of the impact of the ionic metals, corresponding to the amount of metal dissolved from 100 mg/L NPs, showed a similar toxic effect to the one observed for the respective NP supernatant (Supplementary Fig. S4), which confirmed that the impact of the NP supernatant was related to the release of the ions by the NPs.

Possible cellular targets of NPs

To evaluate the possible cytotoxic effects of the NPs, the cell membrane integrity and the metabolic activity of yeast cells exposed for 24 h to NPs, in MES buffer, were assessed.

Membrane integrity was evaluated using a dye (PI) exclusion assay: cells with an intact plasma membrane are not able to accumulate PI; they were PI negative cells (Supplementary Fig. S5) (Hewitt and Nebe-Von-Caron 2001). All NPs studied, up to 100 mg/L, did not provoke a significant modification of plasma membrane integrity, as ~ 100% of cells remained PI negative (Fig. 4a).
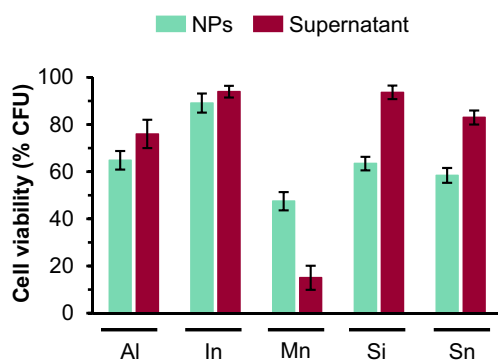
Fig. 3 Comparison of the effect of the nanoparticles or the respective supernatants on yeast cells. Yeasts were exposed for 24 h to the different NPs (100 mg/L), in MES buffer, or to the respective supernatants. Cell viability was evaluated by colony forming unit (CFU) counting. The data are presented as mean values from at least three independent experiments performed in duplicate ($n \geq 6$); standard deviations are presented (vertical error bars)

Metabolic health of yeast cells was assessed using a FUN-1 dye processing assay (Millard et al. 1997) and a fluorescein diacetate (FDA)–based cell esterase activity assay (Breeuwer et al. 1995). Metabolically active cells are able to process FUN-1 dye, forming cylindrical intravacuolar structures (CIVS) (orange-red structures) (Supplementary Fig. S6). With the exception of In_2O_3, the NPs studied induced a small but significant reduction of the % of cells with the ability to process the FUN-1 dye (Fig. 4b). Metabolic active cells were able to hydrolyse FDA (FDA+ cells) (Supplementary Fig. S7). The exposure of yeast cells to MOx NPs caused a reduction of the percentage of FDA-positive cells, except for In_2O_3 (Fig. 4c). The nonfluorescent FDA substrate is hydrolysed, by the action of nonspecific intracellular esterases, into a fluorescent product (fluorescein) and two acetate molecules (Breeuwer et al. 1995). The decrease of the green fluorescence can be used as an indicator of the reduction of esterase activity. The quantification of green fluorescence exhibited by yeast cells loaded with FDA and exposed to MOx NPs revealed that Al_2O_3 and Mn_3O_4 induced the higher reduction of esterase activity, followed by SnO_2 and SiO_2 (Fig. 4d). All together, these results indicate that the exposure to all NPs studied, except In_2O_3, induce a reduction of the metabolic activity in yeasts, in the absence of loss of membrane integrity.

Relationship between the ROS generation and the NPs cytotoxicity

The ability of NPs and/or their respective metal ions to generate ROS in abiotic conditions (cell free) was evaluated. For this end, a test was performed in which the NPs at 100 mg/L were incubated in MES buffer, for 24 h. ROS generation was evaluated using the general redox sensor H_2DCFDA, deacetylated (H_2DCF) (Tarpey et al. 2004; von Moos et al. 2016). The evaluated NPs were not able to generate ROS under abiotic conditions (Fig. 5a).

Yeast cells exposed to all NPs (except In_2O_3), for 24 h, presented a significant accumulation of intracellular ROS (Fig. 5b and Supplementary Fig. S8).

To test whether ROS accumulation was the main cause of cytotoxicity induced by the NPs, yeast cells were exposed to NPs in the presence of L-ascorbic acid (AA), a known free radical scavenger agent (Arrigoni and De Tullio 2002; Nimse and Pal 2015). Subsequently, the levels of intracellular ROS, metabolic activity and cell viability were assessed. Yeast cells co-exposed to NPs and AA presented a significant reduction of the intracellular level of ROS (Fig. 5b). For all NPs, except SiO_2, the intracellular levels of ROS of the yeasts co-exposed to the NPs and AA were not significantly different from the control (Fig. 5b). The co-exposure to AA practically restored the survival (Fig. 5c) and the metabolic activity (Fig. 5d) of yeast cells incubated with NPs. Together, these results strongly support the possibility that the toxicity exerted by the MOx

Fig. 4 Influence of the nanoparticles on membrane integrity and metabolic activity of yeast cells. Yeasts were exposed for 24 h to 100 mg/L of the different NPs in MES buffer; control: cells incubated in MES buffer in the absence of NPs. **a** Membrane integrity assessed by propidium iodide (PI) exclusion assay. **b, c** Quantification of the percentage of metabolically active cells; yeasts were stained with FUN-1 or FDA, respectively. **d** Assessment of esterase activity by the hydrolysis of FDA. The data are presented as mean values from at least three independent experiments performed in duplicate ($n \geq 6$); standard deviations are presented (vertical error bars). Mean values are significantly different: $*P < 0.05$ in comparison with untreated cells (control); unpaired t test
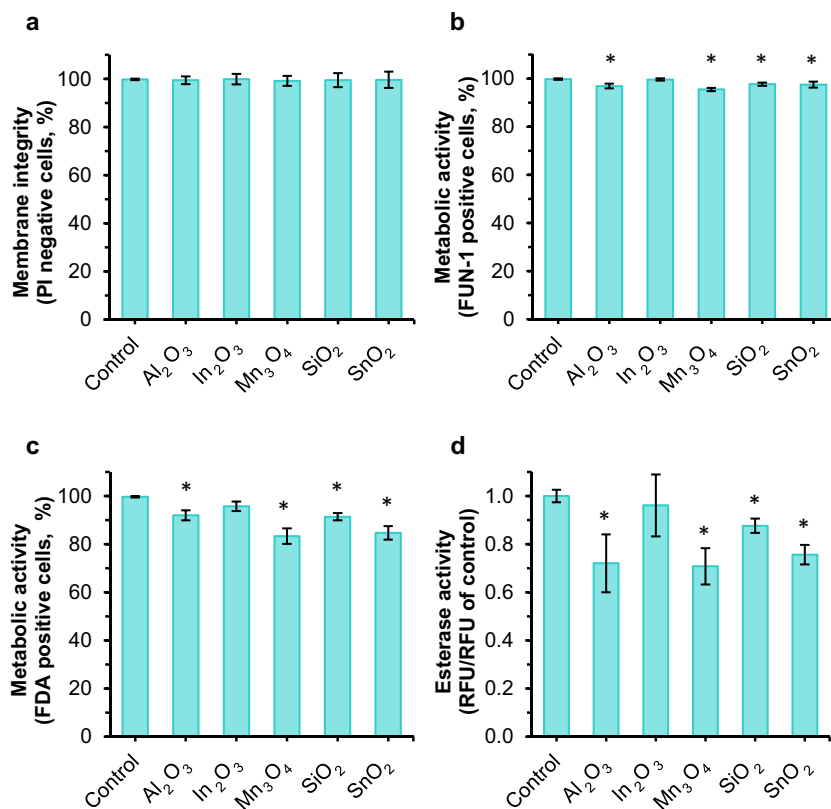
studied, on yeast cells, can be attributed, mainly, to the induction of intracellular accumulation of ROS.

Discussion

MOx NPs accounted for the largest share of the total NPs market. In the last decade, an exponential use of this type of nanomaterials, in the most varied daily products, was observed (Corr 2012). However, the increased use of MOx NPs has also raised concerns about the possible toxic impacts of these nanomaterials.

Physicochemical characterization of the NPs is essential to understand their behaviour and toxicity. In both media tested (MES buffer and YEP broth), the hydrodynamic size increased over time (Fig. 1a) while a reduction of the zeta potential values was observed (Fig. 1b). These low zeta potential values indicated that the NPs were instable in aqueous suspension, having tendency to form agglomerates (Hanaor et al. 2012). This effect was particularly evident in MES buffer where the agglomeration of the NPs could be observed, with the naked eye, in the Erlenmeyer flasks (Supplementary Fig. S1). The properties of these MOx NPs in different aqueous media, such as Dulbecco's modified Eagle medium, OECD algae medium and Luria-Bertani medium, were described in the literature. Similar zeta potential values to those here presented for In_2O_3 (Ahamed et al. 2017), Mn_3O_4 and SiO_2

(Ivask et al. 2015), as well as similar Z-average diameter for Al_2O_3 (Park et al. 2016), Mn_3O_4 (Ivask et al. 2015), SiO_2 (Bondarenko et al. 2016) and SnO_2 NPs (Chavez-Calderon et al. 2016), were reported. The MOx NPs studied presented a low solubility ($< 8\%$) in YEP or MES buffer (Supplementary Table S2). This poor solubility is in agreement with the data described in the literature. In fact, the amount of metal(loid)s released from the NPs, here presented, is of the same order of magnitude of the values reported for In_2O_3 (Bomhard 2018; Jeong et al. 2016), Mn_3O_4 (Ivask et al. 2015), SiO_2 (Van Hoecke et al. 2008) and SnO_2 NPs (Chavez-Calderon et al. 2016).

All NPs studied did not provoke yeast growth inhibition, up to 100 mg/L, when incubated in a protein-rich medium (YEP) (Fig. 2a). It is described that proteins form complexes with NPs, leading to a protein "corona" that defines the biological properties of the NPs (Cedervall et al. 2007; Kharazian et al. 2016). Probably, the formation of protein-coated NPs leads to the reduction of their toxicity, as it was described with other MOx NPs and cell models (Nguyen and Lee 2017). In addition, the metals released by the NPs (Fig. 1c) should be, most likely, complexed by YEP components, which reduce their bioavailability and consequently their toxicity. Consistent with this possibility, it was found that 24-h EC_{50} values of metals in YEP were about ten times higher than those observed in MES buffer (Supplementary Table S3), where no metal complexation occurs (Ferreira et al. 2015).
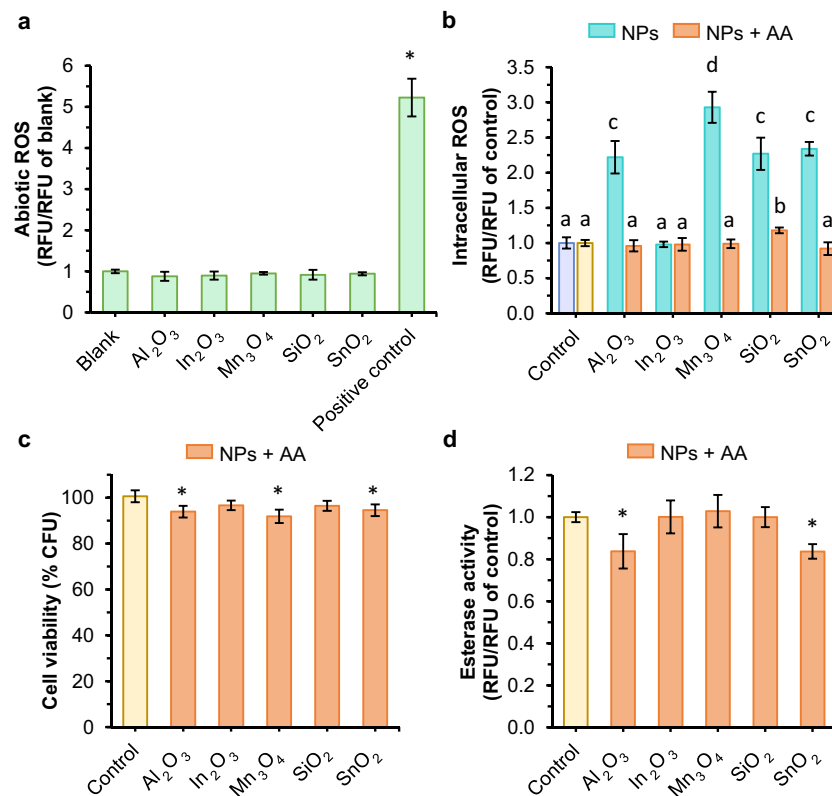
Fig. 5 L-Ascorbic acid reverts the toxic effects induced by the nanoparticles on yeast cells. **a** Assessment of the possible pro-oxidant effect of MOx NPs. NPs at 100 mg/L were incubated with H_2DFC in MES buffer, for 24 h. Blank and positive control were obtained by incubating the H_2DCF probe in MES buffer or with 26 μmol/L H_2O_2, respectively. **b** Evaluation of the oxidative stress induced by MOx NPs. Yeast cells were incubated with 100 mg/L NPs, in MES buffer for 24 h, without (NPs) or with 10 mmol/L L-ascorbic acid (NPs + AA); control: cells incubated in MES buffer in the absence of NPs, without (light blue) or with AA (light orange). Levels of intracellular ROS were quantified using H_2DCFDA. **c**, **d** Yeast cells co-exposed to 100 mg/L MOx NPs and

10 mmol/L AA, in MES buffer, for 24 h; control: cells incubated in MES buffer, with AA, in the absence of NPs. **c** Evaluation of cell viability by colony forming unit (CFU) counting. **d** Metabolic activity assessed through the hydrolysis of FDA. The data are presented as mean values from at least three independent experiments performed in duplicate ($n \geq$ 6); standard deviations are presented (vertical error bars). **a**, **c**, **d** Mean values are significantly different: $*P < 0.05$ in comparison with untreated cells (control); unpaired t test. **b** Means with different letters are significantly different ($P < 0.05$); one-way ANOVA followed by Tukey-Kramer multiple comparison method

Except for In_2O_3, where no toxic effects on yeast cells were observed, all other NPs studied induced a loss of cell viability in a dose-dependent manner (Fig. 2c). Regarding the causes that may induce NPs toxicity, the analysis of the effect of NPs and the respective supernatants (Fig. 3) raises different possibilities. In the case of SiO_2, the toxicity over yeast cells was most likely mainly caused by the NPs themselves, since the supernatant had no impact on cell viability (Fig. 3). A similar observation was reported when the *Photobacterium phosphoreum* was exposed to Fe_2O_3, Co_3O_4, Cr_2O_3 and NiO NPs (Wang et al. 2016). The toxicity of Al_2O_3 and SnO_2 NPs could be attributed to both the NPs and the respective released ions (Fig. 3). A similar result was described when the bacterium *E. coli* was exposed to Al_2O_3 NPs (Simon-Deckers et al. 2009). The loss of yeast cell viability induced by Mn_3O_4 NPs could be mainly caused by the released Mn ions, since the contribution of the Mn_3O_4 NPs to the toxicity could be, practically, neglected (Fig. 3). A similar effect was

described when human lung epithelial cells were exposed to Mn_3O_4 NPs (Ivask et al. 2015).

All NPs studied did not have any pro-oxidant effect (ROS generation in abiotic conditions) (Fig. 5a). These results are compatible with the fact that Al_2O_3 and SnO_2 are considered redox-inactive (Chemicals 2018a, b). In the case of Mn_3O_4 NPs, although considered redox-active (Urner et al. 2014), in the concentration tested, these NPs were unable to oxidized H_2DCF. In the present work, it was observed that Al_2O_3, Mn_3O_4, SiO_2 and SnO_2 NPs induced a significant intracellular accumulation of ROS in yeasts (Fig. 5b). Due to the absence of a pro-oxidant effect of the NPs, it can be deduced that the ROS presented by yeast cells were intracellularly generated. The triggering of OS on yeast cells by the MOx NPs studied (except by In_2O_3) is in agreement with the literature, which describes the ability of these NPs to induce OS in different cell models. Thus, it was reported that Al_2O_3 caused OS in plant wheat roots (*Triticum aestivum*) (Yanik and Vardar 2018) and

in human lymphocytes (Rajiv et al. 2016). Mn_3O_4 NPs induced elevated ROS levels in rat alveolar macrophages (Urner et al. 2014) and alveolar epithelial cells (Frick et al. 2011), and SiO_2 NPs provoked the generation of ROS in different cell lines: lymphocyte (Azimipour et al. 2018), intestinal cells (Setyawati et al. 2015), lung and bronchial epithelial cells (Eom and Jinhee Cho 2011; Manke et al. 2013).

Main targets of ROS include membrane lipids, nucleic acids and ROS-susceptible proteins (Avery 2011). The levels of intracellular ROS in yeast cells exposed for 24 h to all NPs studied were not enough to induce the loss of cell membrane integrity (Fig. 4a). Similarly, it was described that SiO_2 did not have any impact on membrane integrity of algal cells *Scenedesmus obliquus* (Liu et al. 2018). Although it was reported the disruption of cell membrane in yeasts exposed to Al_2O_3 NPs (Garcia-Saucedo et al. 2011) or Mn_2O_3 (Otero-Gonzalez et al. 2013), both results were observed in the presence of 1 g/L NPs, which corresponded to a concentration ten times higher than the one used in the present study.

The incubation of yeast cells with Al_2O_3, Mn_3O_4, SiO_2 or SnO_2 induced a small, but significant, loss of the metabolic activity (Fig. 4b–d). A decrease of the metabolic activity due to the exposure to Mn_3O_4 NPs was observed in different animal cells (Titma et al. 2016). The reduction of the hydrolytic activity of the esterases could be due to the oxidation of this enzyme as consequence of the intracellular ROS accumulation. It was reported that protein oxidation can occur by different modes, which includes cleavage of peptide bonds and oxidation of sensitive amino acid residues, such as those containing aromatic side chain or sulfhydryl groups (Cecarini et al. 2007). Compatible with the possibility that OS may have been responsible for the reduction of yeast hydrolytic activity, it was observed that the simultaneous incubation of the cells with NPs and AA almost (SiO_2) or completely abrogated (Al_2O_3, Mn_3O_4 and SnO_2) the OS (Fig. 5b) and restored the esterase activity (Mn_3O_4 and SiO_2) of yeast cells (Fig. 5d). In addition, yeast survival was completely (SiO_2) or almost completely restored (Al_2O_3, Mn_3O_4 and SnO_2) (Fig. 5c) when the cells were co-exposed to NPs and AA. The reversibility of the toxic effects, induced by the MOx NPs, due to the presence of AA, strongly indicates that OS is, most likely, the main contributor of the cytotoxicity observed in yeast cells.

In conclusion, the NPs tested when suspended in aqueous media displayed, in a general way, a negative charge, agglomerated (except SnO_2 in YEP), were almost insoluble (dissolution < 8%) and were unable to generate ROS in abiotic conditions. In_2O_3 NPs did not provoke any detectable toxic effect on yeast cells up to 100 mg/L. Al_2O_3, Mn_3O_4, SiO_2 and SnO_2 NPs induced the loss of yeast cell viability. The comparative analysis of the effect of the MOx NPs and the corresponding supernatants suggested
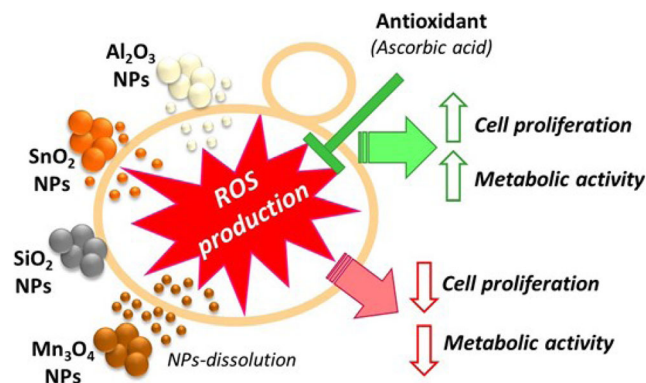
Fig. 6 Pictorial representation of the toxic effects of the nanoparticles studied. Source of NPs toxicity: SiO_2—NPs themselves; Al_2O_3 and SnO_2—NPs and respective released ions; Mn_3O_4—release of Mn ions. All NPs induced the generation of intracellular ROS, which was accompanied by a loss of cell proliferation capacity and metabolic activity. ROS scavenging, due to co-exposure to acid ascorbic, quenched intracellular ROS and significantly restored cell viability and metabolic activity

that the SiO_2 toxicity was mainly caused by the NPs themselves, Al_2O_3 and SnO_2 toxic effects could be attributed to both the NPs and the respective released ions and Mn_3O_4 harmfulness could be mainly produced by the released ions (Fig. 6). These NPs also induced the loss of metabolic activity and intracellular ROS accumulation. The cytotoxic effects were observed at sub-lethal concentrations, since NPs up to 100 mg/L did not induce the loss of plasma membrane integrity of yeasts. The co-incubation of yeast cells with the NPs and AA quenched intracellular ROS and reverted the NPs toxicity (nearly restored cell survival and metabolic activity), evidencing that the intracellular accumulation of ROS constitutes the main cause of the cytotoxicity experienced by yeasts treated with Al_2O_3, Mn_3O_4, SiO_2 and SnO_2 NPs (Fig. 6). This study showed that OS constitutes an important mechanism whereby MOx NPs exert the toxicity in yeast cells. The present work contributes to the characterization of the mechanisms of toxicity associated with MOx NPs and alerts for the possible negative impact of the use of these nanomaterials. The data here obtained could be useful to support the development of further regulations related with the risk reduction due to the exposure to the NPs studied.

Compliance with ethical standards

This article does not contain any studies with human participants or animals performed by any of the authors.

Conflict of interest   The authors declare that they have no conflict of interest.

References

Ahamed M, Akhtar MJ, Khan MAM, Alhadlaq HA, Aldalbahi A (2017) Nanocubes of indium oxide induce cytotoxicity and apoptosis through oxidative stress in human lung epithelial cells. Colloids Surf B: Biointerfaces 156:157–164. https://doi.org/10.1016/j.colsurfb.2017.05.020

Andreescu S, Ornatska M, Erlichman JS, Estevez A, Leiter JC (2012) Biomedical applications of metal oxide nanoparticles. In: Matijević E (ed) Fine particles in medicine and pharmacy. Springer, Boston, MA, pp 57–100

Arrigoni O, De Tullio MC (2002) Ascorbic acid: much more than just an antioxidant. Biochim Biophys Acta 1569(1–3):1–9. https://doi.org/10.1016/s0304-4165(01)00235-5

Aruoja V, Pokhrel S, Sihtmae M, Mortimer M, Madler L, Kahru A (2015) Toxicity of 12 metal-based nanoparticles to algae, bacteria and protozoa. Environ Sci Nano 2(6):630–644. https://doi.org/10.1039/c5en00057b

Avery SV (2011) Molecular targets of oxidative stress. Biochem J 434: 201–210. https://doi.org/10.1042/bj20101695

Azimipour S, Ghaedi S, Mehrabi Z, Ghasemzadeh SA, Heshmati M, Barikrow N, Attar F, Falahati M (2018) Heme degradation and iron release of hemoglobin and oxidative stress of lymphocyte cells in the presence of silica nanoparticles. Int J Biol Macromol 118:800–807. https://doi.org/10.1016/j.ijbiomac.2018.06.128

AzoNano (2018) Indium oxide (In_2O_3) nanoparticles—properties, applications https://www.azonano.com/article.aspx?ArticleID=3331. Accessed 15 October 2018

Bomhard EM (2018) The toxicology of indium oxide. Environ Toxicol Pharmacol 58:250–258. https://doi.org/10.1016/j.etap.2018.02.003

Bondarenko OM, Heinlaan M, Sihtmae M, Ivask A, Kurvet I, Joonas E, Jemec A, Mannerstrom M, Heinonen T, Rekulapelly R, Singh S, Zou J, Pyykko I, Drobne D, Kahru A (2016) Multilaboratory evaluation of 15 bioassays for (eco)toxicity screening and hazard ranking of engineered nanomaterials: FP7 project NANOVALID. Nanotoxicology 10(9):1229–1242. https://doi.org/10.1080/17435390.2016.1196251

Breeuwer P, Drocourt JL, Bunschoten N, Zwietering MH, Rombouts FM, Abee T (1995) Characterization of uptake and hydrolysis of fluorescein diacetate and carboxyfluorescein diacetate by intracellular esterases in Saccharomyces cerevisiae, which result in accumulation of fluorescent product. Appl Environ Microbiol 61(4):1614–1619

Cecarini V, Gee J, Fioretti E, Amici M, Angeletti M, Eleuteri AM, Keller JN (2007) Protein oxidation and cellular homeostasis: emphasis on metabolism. Biochim Biophys Acta 1773(2):93–104. https://doi.org/10.1016/j.bbamcr.2006.08.039

Cedervall T, Lynch I, Lindman S, Berggard T, Thulin E, Nilsson H, Dawson KA, Linse S (2007) Understanding the nanoparticle-protein corona using methods to quantify exchange rates and affinities of proteins for nanoparticles. Proc Natl Acad Sci U S A 104(7):2050–2055. https://doi.org/10.1073/pnas.0608582104

Chai HK, Yao J, Sun JJ, Zhang C, Liu WJ, Zhu MJ, Ceccanti B (2015) The effect of metal oxide nanoparticles on functional bacteria and metabolic profiles in agricultural soil. Bull Environ Contam Toxicol 94(4):490–495. https://doi.org/10.1007/s00128-015-1485-9

Chavez-Calderon A, Paraguay-Delgado F, Orrantia-Borunda E, Luna-Velasco A (2016) Size effect of SnO_2 nanoparticles on bacteria toxicity and their membrane damage. Chemosphere 165:33–40. https://doi.org/10.1016/j.chemosphere.2016.09.003

Chemicals (2018a) Aluminium oxide. https://cameochemicals.noaa.gov/chemical/16127. Accessed 6 August 2018

Chemicals (2018b) Tin (IV) oxide. https://cameochemicals.noaa.gov/chemical/25077. Accessed 6 August 2018

Corr SA (2012) Metal oxide nanoparticles. In: O'Brien P (ed) Nanoscience: volume 1: nanostructures through chemistry. The Royal Society of Chemistry, London, pp 180–207

dos Santos SC, Teixeira MC, Cabrito TR, Sa-Correia I (2012) Yeast toxicogenomics: genome-wide responses to chemical stresses with impact in environmental health, pharmacology, and biotechnology. Front Genet 3(63):1–17. https://doi.org/10.3389/fgene.2012.00063

Eom H-J, Jinhee Cho J (2011) SiO_2 nanoparticles induced cytotoxicity by oxidative stress in human bronchial epithelial cell, Beas-2B. Environ Health Toxicol 26:1–7

Fei J, Li J (2010) Metal oxide nanomaterials for water treatment. In: Kumar CSSR (ed) Nanotechnologies for the life sciences: nano-structured oxides, vol 2. Wiley-VCH Verlag GmbH & Co. KGaA, Weinheim, pp 287–315

Ferreira CMH, Pinto ISS, Soares EV, Soares H (2015) (Un)suitability of the use of pH buffers in biological, biochemical and environmental studies and their interaction with metal ions—a review. RSC Adv 5(39):30989–31003. https://doi.org/10.1039/c4ra15453c

Frick R, Müller-Edenborn B, Schlicker A, Rothen-Rutishauser B, Raemy DO, Günther D, Hattendorf B, Stark W, Beck-Schimmer B (2011) Comparison of manganese oxide nano-particles and manganese sulfate with regard to oxidative stress, uptake and apoptosis in alveolar epithelial cells. Toxicol Lett 205(2):163–172. https://doi.org/10.1016/j.toxlet.2011.05.1037

Garcia-Saucedo C, Field JA, Otero-Gonzalez L, Sierra-Alvarez R (2011) Low toxicity of HfO_2, SiO_2, Al_2O_3 and CeO_2 nanoparticles to the yeast, Saccharomyces cerevisiae. J Hazard Mater 192(3):1572–1579. https://doi.org/10.1016/j.jhazmat.2011.06.081

Goffeau A, Barrell BG, Bussey H, Davis RW, Dujon B, Feldmann H, Galibert F, Hoheisel JD, Jacq C, Johnston M, Louis EJ, Mewes HW, Murakami Y, Philippsen P, Tettelin H, Oliver SG (1996) Life with 6000 genes. Science 274(5287):546–567. https://doi.org/10.1126/science.274.5287.546

Hanaor D, Michelazzi M, Leonelli C, Sorrell CC (2012) The effects of carboxylic acids on the aqueous dispersion and electrophoretic deposition of ZrO_2. J Eur Ceram Soc 32(1):235–244. https://doi.org/10.1016/j.jeurceramsoc.2011.08.015

Hartmann NB, Engelbrekt C, Zhang JD, Ulstrup J, Kusk KO, Baun A (2013) The challenges of testing metal and metal oxide nanoparticles in algal bioassays: titanium dioxide and gold nanoparticles as case studies. Nanotoxicology 7(6): 1082–1094. https://doi.org/10.3109/17435390.2012.710657

Hewitt CJ, Nebe-Von-Caron G (2001) An industrial application of multiparameter flow cytometry: assessment of cell physiological state and its application to the study of microbial fermentations. Cytometry 44(3):179–187. https://doi.org/10.1002/1097-0320(20010701)44:3<179::aid-cyto1110>3.0.co;2-d

Hirner AV, Flaßbeck D (2005) Speciation of silicon. In: Cornelis R, Crews H, Caruso J, Heumann KG (eds) Handbook of elemental

speciation II – species in the environment, food, medicine and occupational health. Wiley, Chichester, pp 366–377

Iler RK (1978) The occurrence, dissolution, and deposition of silica. In: Iler RK (ed) The chemistry of silica: solubility, polymerization, colloid and surface properties, and biochemistry. Wiley, New York, pp 3–115

Ivask A, Titma T, Visnapuu M, Vija H, Kakinen A, Sihtmae M, Pokhrel S, Madler L, Heinlaan M, Kisand V, Shimmo R, Kahru A (2015) Toxicity of 11 metal oxide nanoparticles to three mammalian cell types in vitro. Curr Top Med Chem 15(18):1914–1929. https://doi.org/10.2174/1568026615666150506150109

Jeong J, Kim J, Seok SH, Cho WS (2016) Indium oxide (In_2O_3) nanoparticles induce progressive lung injury distinct from lung injuries by copper oxide (CuO) and nickel oxide (NiO) nanoparticles. Arch Toxicol 90(4):817–828. https://doi.org/10.1007/s00204-015-1493-x

Karathia H, Vilaprinyo E, Sorribas A, Alves R (2011) Saccharomyces cerevisiae as a model organism: a comparative study. PLoS One 6(2):e16015

Kharazian B, Hadipour NL, Ejtehadi MR (2016) Understanding the nanoparticle-protein corona complexes using computational and experimental methods. Int J Biochem Cell Biol 75:162–174. https://doi.org/10.1016/j.biocel.2016.02.008

Klaine SJ, Edgington A, Seda B (2013) Nanomaterials in the environment. In: Férard J-F, Blaise C (eds) Encyclopedia of aquatic ecotoxicology. Springer Publishers, Dordrecht, pp 767–779

Laurent S, Boutry S, Muller RN (2018) Metal oxide particles and their prospects for applications. In: Mahmoudi M, Laurent S (eds) Iron oxide nanoparticles for biomedical applications: synthesis, functionalization and application. Elsevier, London, pp 3–42

Li KG, Chen Y, Zhang W, Pu ZC, Jiang L, Chen YS (2012) Surface interactions affect the toxicity of engineered metal oxide nanoparticles toward Paramecium. Chem Res Toxicol 25(8):1675–1681. https://doi.org/10.1021/tx300151y

Liu YH, Wang S, Wang Z, Ye N, Fang H, Wang DG (2018) TiO_2, SiO_2 and ZrO_2 nanoparticles synergistically provoke cellular oxidative damage in freshwater microalgae. Nanomaterials 8(2):95

Manke A, Wang L, Rojanasakul Y (2013) Mechanisms of nanoparticle-induced oxidative stress and toxicity. Biomed Res Int 2013:1–15

McGee CF, Storey S, Clipson N, Doyle E (2017) Soil microbial community responses to contamination with silver, aluminium oxide and silicon dioxide nanoparticles. Ecotoxicology 26(3):449–458. https://doi.org/10.1007/s10646-017-1776-5

Millard PJ, Roth BL, Thi HPT, Yue ST, Haugland RP (1997) Development of the FUN-1 family of fluorescent probes for vacuole labeling and viability testing of yeasts. Appl Environ Microbiol 63(7):2897–2905

Nanotech (2015) Aluminium oxide: forecast from 2010 to 2025 nanoparticles. Future Markets Inc., Edinburgh

Nguyen VH, Lee BJ (2017) Protein corona: a new approach for nanomedicine design. Int J Nanomedicine 12:3137–3151. https://doi.org/10.2147/ijn.s129300

Nimse SB, Pal D (2015) Free radicals, natural antioxidants, and their reaction mechanisms. RSC Adv 5(35):27986–28006. https://doi.org/10.1039/c4ra13315c

OECD (2011) Test N° 201: freshwater alga and cyanobacteria, growth inhibition test. OECD guidelines for the testing of chemicals, Section 2. OECD Publishing, Paris. https://doi.org/10.1787/9789264069923-en

OECD (2017) Test n° 318: dispersion stability of nanomaterials in simulated environmental media. OECD guidelines for the testing of chemicals, section 3. OECD Publishing, Paris. https://doi.org/10.1787/9789264284142-en

Otero-Gonzalez L, Garcia-Saucedo C, Field JA, Sierra-Alvarez R (2013) Toxicity of TiO_2, ZrO_2, Fe^0, Fe_2O_3, and Mn_2O_3 nanoparticles to the

yeast, Saccharomyces cerevisiae. Chemosphere 93(6):1201–1206. https://doi.org/10.1016/j.chemosphere.2013.06.075

Park EJ, Lee GH, Yoon C, Jeong U, Kim Y, Cho MH, Kim DW (2016) Biodistribution and toxicity of spherical aluminium oxide nanoparticles. J Appl Toxicol 36(3):424–433

Perry CC, Belton D, Shafran K (2003) Studies of biosilicas; structural aspects, chemical principles, model studies and the future. In: Müller WEG (ed) Silicon biomineralization: biology-biochemistry-molecular biology-biotechnology. Progress in molecular and subcellular biology. Springer-Verlag, Berlin, pp 269–299

Rajiv S, Jerobin J, Saranya V, Nainawat M, Sharma A, Makwana P, Gayathri C, Bharath L, Singh M, Kumar M, Mukherjee A, Chandrasekaran N (2016) Comparative cytotoxicity and genotoxicity of cobalt (II, III) oxide, iron (III) oxide, silicon dioxide, and aluminum oxide nanoparticles on human lymphocytes in vitro. Hum Exp Toxicol 35(2):170–183. https://doi.org/10.1177/0960327115579208

Report (2018) Market research report: nanomaterials. https://www.alliedmarketresearch.com/press-release/nanomaterials-market.html. Accessed 15 October 2018

Research (2017) Global markets for nanocomposites, nanoparticles, nanoclays, and nanotubes. http://www.bccresearch.com/market-research/nanotechnology/nanocomposites-nanoparticles-nantubes-market-report-nan021g.html. Accessed 23 January 2017

Research (2018) Indium market size by product: global industry report 2018–2025. https://www.grandviewresearch.com/industry-analysis/indium-market. Accessed 15 October 2018

Setyawati MI, Tay CY, Leong DT (2015) Mechanistic investigation of the biological effects of SiO_2, TiO_2, and ZnO nanoparticles on intestinal cells. Small 11(28):3458–3468. https://doi.org/10.1002/smll.201403232

Simon-Deckers A, Loo S, Mayne-L'Hermite M, Herlin-Boime N, Menguy N, Reynaud C, Gouget B, Carriere M (2009) Size-, composition- and shape-dependent toxicological impact of metal oxide nanoparticles and carbon nanotubes toward bacteria. Environ Sci Technol 43(21):8423–8429. https://doi.org/10.1021/es9016975

Sousa CA, Soares H, Soares EV (2018) Nickel oxide (NiO) nanoparticles disturb physiology and induce cell death in the yeast Saccharomyces cerevisiae. Appl Microbiol Biotechnol 102(6):2827–2838. https://doi.org/10.1007/s00253-018-8802-2

Tarpey MM, Wink DA, Grisham MB (2004) Methods for detection of reactive metabolites of oxygen and nitrogen: in vitro and in vivo considerations. Am J Phys Regul Integr Comp Phys 286(3):R431–R444. https://doi.org/10.1152/ajpregu.00361.2003

Tian Z-Y, Kouotou PM, Bahlawane N, Ngamou PHT (2013) Synthesis of the catalytically active Mn_3O_4 spinel and its thermal properties. J Phys Chem C 117(2):6218–6224

Titma T, Shimmo R, Siigur J, Kahru A (2016) Toxicity of antimony, copper, cobalt, manganese, titanium and zinc oxide nanoparticles for the alveolar and intestinal epithelial barrier cells in vitro. Cytotechnology 68(6):2363–2377. https://doi.org/10.1007/s10616-016-0032-9

Urner M, Schlicker A, Z'Graggen BR, Stepuk A, Booy C, Buehler KP, Limbach L, Chmiel C, Stark WJ, Beck-Schimmer B (2014) Inflammatory response of lung macrophages and epithelial cells after exposure to redox active nanoparticles: effect of solubility and antioxidant treatment. Environ Sci Technol 48(23):13960–13968. https://doi.org/10.1021/es504011m

Van Hoecke K, De Schamphelaere KAC, Van der Meeren P, Lucas S, Janssen CR (2008) Ecotoxicity of silica nanoparticles to the green alga Pseudokirchneriella subcapitata: importance of surface area. Environ Toxicol Chem 27(9):1948–1957. https://doi.org/10.1897/07-634.1

von Moos N, Koman VB, Santschi C, Martin OJF, Maurizi L, Jayaprakash A, Bowen P, Slaveykova VI (2016) Pro-oxidant effects of nano-TiO$_2$ on *Chlamydomonas reinhardtii* during short-term exposure. RSC Adv 6(116):115271–115283. https://doi.org/10.1039/c6ra16639c

Wang DL, Lin ZF, Wang T, Yao ZF, Qin MN, Zheng SR, Lu W (2016) Where does the toxicity of metal oxide nanoparticles come from: the nanoparticles, the ions, or a combination of both? J Hazard Mater 308:328–334. https://doi.org/10.1016/j.jhazmat.2016.01.066

Yanik F, Vardar F (2018) Oxidative stress response to aluminum oxide (Al$_2$O$_3$) nanoparticles in *Triticum aestivum*. Biologia 73(2):129–135. https://doi.org/10.2478/s11756-018-0016-7